

K^-p INTERACTIONS AT 11 GeV/c: NEW RESULTS
ON STRANGE MESON SYSTEMS*

Blair N. Ratcliff
Stanford Linear Accelerator Center,
Stanford University, California

ABSTRACT

The status of our programmatic study of states containing a strange quark is briefly reviewed. An 11 GeV/c K^-p experiment run on the LASS spectrometer at SLAC is discussed and preliminary results presented for several inelastic channels based on approximately one half of the available data sample. In addition, new results utilizing the full statistics of the experiment are presented for the elastic $K^- \pi^+$ channel from the $K^- \pi^+ n$ final state. The well established leading $K^*(890)$, $K^*(1435)$, and $K^*(1780)$ resonances are observed, and clear evidence is presented for a new $J^P = 4^+$ resonance at ~ 2070 MeV. Preliminary results from an energy independent partial wave analysis of these data are presented which display unambiguous evidence for resonant structure in the non-leading 0^+ and 1^- waves.

Invited talk presented at
The International Conference on Experimental Meson Spectroscopy
Brookhaven National Laboratory, Upton, New York
April 25-26, 1980

*Work supported by the Department of Energy, contract DE-AC03-76SF00515.

I. INTRODUCTION

During the last several years, we have been engaged in a systematic study of strange quark spectroscopy and reaction dynamics for the production of these states, using the rf separated K^+ beams at SLAC. The physics goals of this program are, in general, to provide a "great leap forward" in our understanding of the K^* (e.g., $s\bar{u}$), and ϕ' ($s\bar{s}$) "strangeonium" mesons, and of the strangeness -2 and -3 hyperons (e.g., ssu). Since nature has provided us with no stable meson or strange baryon targets, these areas have lagged far behind during the rapid progress made in the last decade toward understanding the hadron spectrum.

The first experiment in this series was a 13 GeV K^+ experiment using a forward dipole spectrometer.¹ This experiment was very successful in studying the low mass, low multiplicity states. For example, the two 1^+ Q mesons required by the quark model were observed through a partial wave analysis of the $K\pi\pi$ channel,² and a partial wave analysis of the $K\pi$ channel was also carried out from low mass through the $K^*(1780)$ region.³ However, forward dipole spectrometers have acceptance limitations which hinder their application to higher masses or to higher multiplicity states. We have therefore continued these studies in our current experiment, which uses the LASS spectrometer, to study K^+p interactions at 11 GeV/c.

This experiment triggered on essentially the total charged-inelastic cross section and attained a visible sensitivity of ~ 700 events per μb in most channels. A substantial portion of the events from this experiment has now been passed through the tracking programs and provides the data on which this talk is based. Starting this summer, we will be extending this data sample to over 5 events per nb in a sequel LASS experiment which uses both K^+ and K^- beams at 11 GeV.⁴

II. EXPERIMENT

The experiment I will be discussing today was performed by a collaboration of physicists from SLAC, Carleton University, and the National Research Council of Canada.⁵ The experiment uses the LASS

spectrometer facility which is shown in figure 1. It is serviced by an rf separated beam which can deliver usable kaon fluxes up to 14 GeV/c. LASS contains two large magnets filled with tracking detectors. The first magnet is a superconducting solenoid with a 23 kG field-parallel to the beam direction. This is followed by a 27 kG-m dipole magnet with a vertical field. The solenoid is effective in measuring the interaction products which have large production angles and relatively low momenta. High energy secondaries, tending to stay close to the beam line, are not well measured in the solenoid, but will pass through the dipole for measurement there. Particle identification is provided by Čerenkov counters C1 and C2, and a time of flight (TOF) hodoscope. The trigger for this experiment required two or more charged particles to exit the target and was essentially defined by requiring more than two hits in the full-aperture proportional chamber which immediately followed the target.

The total data sample for this experiment contains some 4×10^7 good events. Analyzing this amount of data clearly requires a substantial amount of computer time and, therefore, calendar time as well. In order to make the full statistics of the experiment available in specific channels relatively early, we split the analysis into two phases. First, we used multiplicity information from the

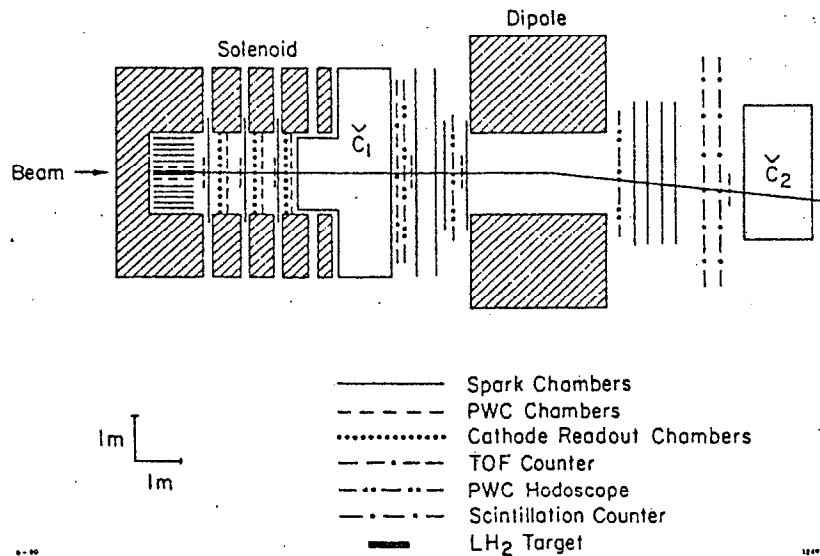


Fig. 1. Plan view of the LASS spectrometer.

proportional chamber system as a software prefilter to select two-prong data from the standard data tapes. The production of this data onto data summary tapes was completed in January of this year. Preliminary physics results from the $K\pi n$ channel based on the full statistics of the experiment are now available, as I will be discussing in a few minutes. At the same time, we have been continuing with the analysis of the multiprong channels using the central computers of SLAC and the NRC. During the last few months, we have also begun production running with the LASS microprocessor system, the 168/E.⁶ The 168/E processors are the result of development efforts to provide the substantial computer analysis power required to handle the data processing load from LASS. They emulate the subset of the instructions of an IBM 370 computer required by a standard FORTRAN-compiled scientific program, so that we are able to run our track finding and fitting programs interchangeably on the central computer or on the emulator. Each 168/E provides about one-half the analysis power of a fully dedicated 370/168 to this experiment. We have been running with a single processor since early January and a two processor system since March. We expect to have six processors in operation by summer with an additional three being added in the fall for processing the data from our sequel experiment. At the present time we have processed over 50 percent of the multiprong data from the present experiment, and expect to finish the production processing by the late summer.

III. MULTIPRONG CHANNELS

Before discussing the $K\pi n$ channel in detail, I would like to briefly describe preliminary results on some selected multiprong channels to indicate the breadth of topics that will be available for study in this experiment. These data are based on partial samples from our present analysis and typically contain some 30 percent of the total statistics of the current experiment.

First of all, even though this is a meson spectroscopy conference, it is hard to resist showing a hyperon state. In spite of the rather complete understanding of baryon spectra in general, the Ξ^*

and Ω^* excited states have remained poorly understood. In particular, only three of the 16 Ξ^* and zero of seven Ω^* states are well established in the otherwise clearly defined baryon supermultiplets. The fundamental reason for this lack of information is that these states can be observed only in production experiments. Their decay topologies are also quite complex so that they have generally been studied only in bubble chamber experiments. The largest of these experiments has a sensitivity of about 100 events per μb so that it produces about 100 Ω^- and a few thousand Ξ^- . The sensitivity of our present experiment is several times this level, and the experiment which is now beginning will increase the sensitivity of these studies by a factor of about 50.

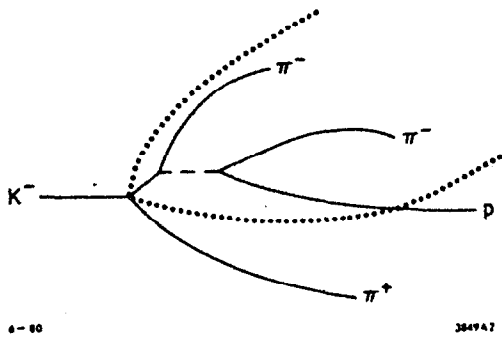


Fig. 2. Schematic of a $\Xi^- \pi^+$ system.

One reconstructs Ξ^- states as indicated in figure 2. A $\pi^- p V^0$ vertex with a Λ invariant mass is combined with a π^- to form a secondary V^- vertex, giving the clear Ξ^- signal shown in figure 3(a). If one then forms combinations of Ξ^- and π^+ at the primary vertex, the invariant mass distribution, figure 3(b), shows strong production of the $\Xi^*(1530)$, as expected.

Let us turn now to the strangeness -1 meson systems. Let me remind you that the goal of meson spectroscopy is not simply to catalogue states in the quark model, but also to confront basic questions about the quark-quark forces, such as understanding the spin and radial excitation dependence of these systems. This effort requires careful study of the classification, level splittings, and mixing of the various states. This, in turn, requires a large amount of data in both elastic and inelastic channels. Indeed, it will often be essential to observe states in several different channels in order to understand them in detail. For example, in the case of the $J^P = 1^-$ $K^*(1650)$, which was observed in two of four solutions through the

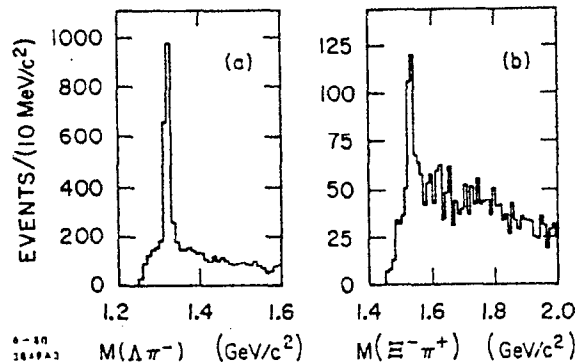


Fig. 3. Invariant mass spectra for inclusive hyperon production. (a) $\Lambda\pi^-$ mass combination. (b) $\Xi^-\pi^+$ mass combination.

partial wave analysis of the $K\pi n$ channel in our 13 GeV experiment,³ it is not clear if it should be classified as a radial excitation or as a non-leading member of the D-wave $q\bar{q}$ triplet. This question can be addressed by measuring the interference between the $K^*(1780)$ and the $K^*(1650)$ in an inelastic final state and determining the relative sign of the couplings. Using a higher symmetry scheme such as SU(6), the classification can then be attempted.

With this as an introduction, let me display a few examples of the present status of our data samples in the inelastic channels. In figure 4(a), we show the invariant $K^0\pi^+\pi^-$ mass from the reaction $K^-p \rightarrow K^0\pi^+\pi^-n$. Clear structures are observed in the 1435 and 1780 mass regions.

There is substantial evidence for "cascade" type decays in this channel as is displayed in figures 4(b-e). Figures 4(b-c) respectively show the $\pi^+\pi^-$ and $K^0\pi^-$ mass combinations to be dominated by ρ and $K^*(890)$. One also sees a smaller amount of $K^*(1435)$ in the $K^0\pi^-$ distribution. If one selects on the ρ and $K^*(890)$ isobars indicated, the invariant mass distributions of figures 4(d) and 4(e) are obtained. In both distributions, structure in the 1435 and 1780 regions is clearly seen, presumably indicative of the expected leading K^* states.

Next, let us turn to the reaction $K^-p \rightarrow K^-\pi^+\pi^-p$. Historically, this reaction has been the most important source of information about the unnatural spin-parity K^* mesons, as Cashmore reviewed for us in

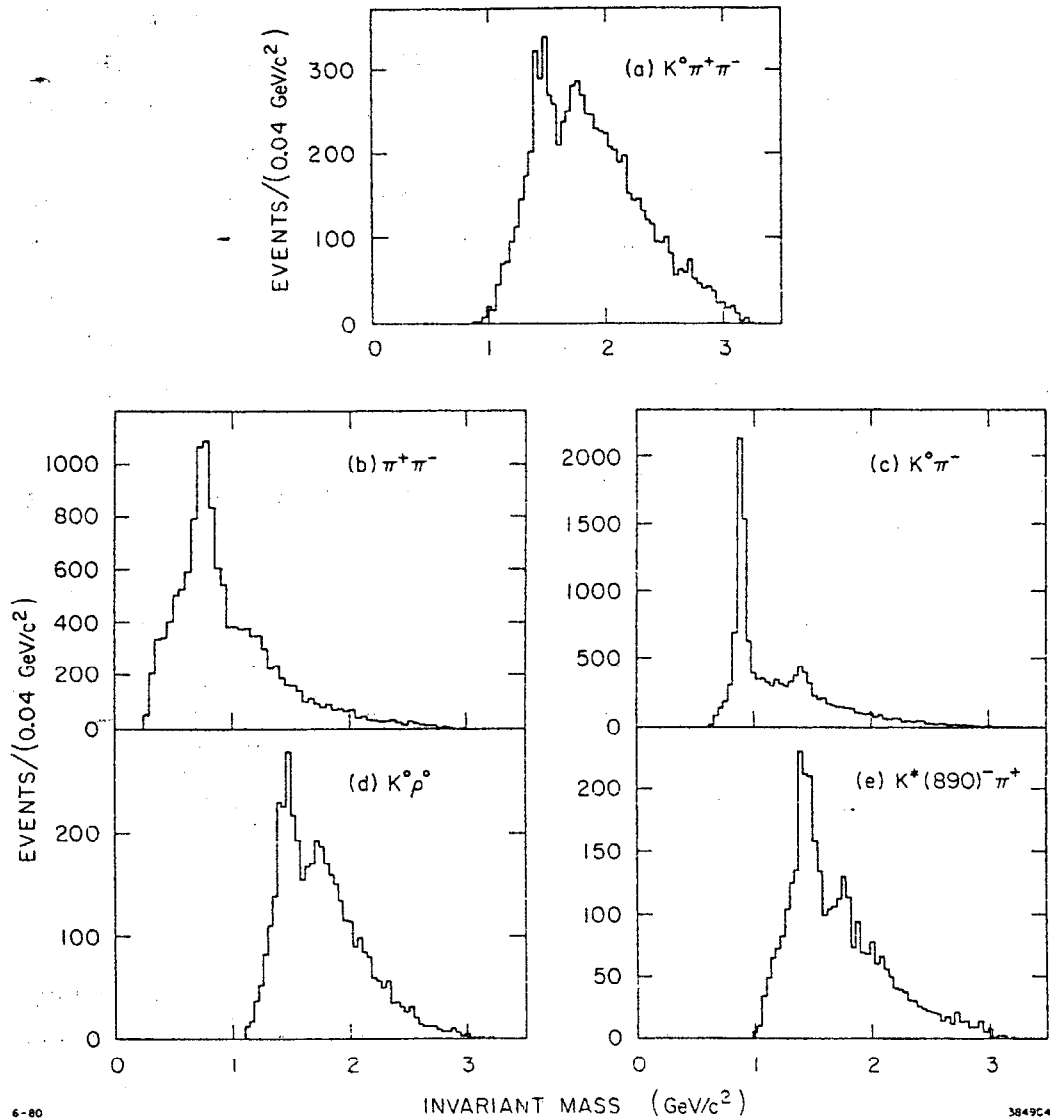


Fig. 4. Invariant mass spectra for the reaction $K^-p \rightarrow K^0\pi^+\pi^-n$. Events selected for $|t| < 0.5 \text{ GeV}^2$, $M(\pi^+n) > 1.34 \text{ GeV}$, and $M(K^0n) > 1.50 \text{ GeV}$. (a) $K^0\pi^+\pi^-$ mass combination. (b) $\pi^+\pi^-$ mass combination. (c) $K^0\pi^-$ mass combination. (d) $K^0\rho^0$ mass combination where $.65 < M_{\pi\pi} < .89 \text{ GeV}$. (e) $K^*(890)\pi$ mass combination where $.81 < M_{K\pi} < .98 \text{ GeV}$.

the previous talk.^{2,7} In order to extract the detailed information required, it is necessary to apply a sophisticated partial wave analysis program to the data. We use the SLAC-LBL approach which directly fits the scattering amplitudes to the data. The present data sample corresponds to about 45 percent of the total data sample and typically

contains 3500 events per 20 MeV bin in the Q region. At the present time, we have analyzed only the region below 1.6 GeV. In general,

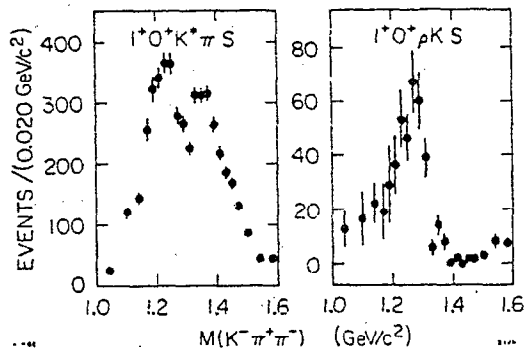


Fig. 5. Preliminary results on the 1^+0^+S wave in the Q region taken from the partial wave analysis of $K^-\pi^+\pi^-$ scattering in the reaction $K^-p \rightarrow K^-\pi^+\pi^-p$

our results are consistent with those from our earlier analysis.² Figure 5 displays the amplitudes for the 1^+0^+S wave $K^*\pi$ and ρK channels which dominate the Q mass region. We see clear structure in both channels, indicating the presence of the two Q mesons previously observed,^{2,7} one with a mass of ~ 1300 MeV coupling mainly to $K\rho$, and the other at ~ 1400 MeV coupling mainly to $K^*\pi$.

IV. THE $K\pi$ ELASTIC CHANNEL

We now turn to an analysis of the natural spin-parity K^* mesons taken from the full experimental statistics on the reaction $K^-p \rightarrow K^-\pi^+n$. The raw data sample for this reaction contains 142,000 events in the invariant $K\pi$ mass region ($M(K\pi)$) between .7 and 2.5 GeV. In figure 6, we see sharp peaks in the invariant mass corresponding

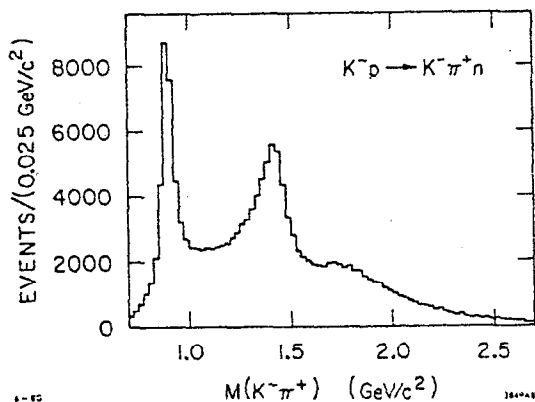


Fig. 6. Invariant $K\pi$ mass distribution from the reaction $K^-p \rightarrow K^-\pi^+n$ with $|t'| < 1.0$ GeV².

to the $K^*(890)$ and $K^*(1435)$ with perhaps a small hint of some structure in the region around 1800 MeV. There is also some asymmetry on the lower side of the $K^*(1435)$ bump hinting, perhaps, at other underlying effects, but in general, little clear evidence for states other than the two well known leading K^* states.

A great deal of interesting structure is hidden in this

plot, however, as becomes evident when we increase its dimensionality. Figure 7 is a computer generated apparent 3-d image where the two

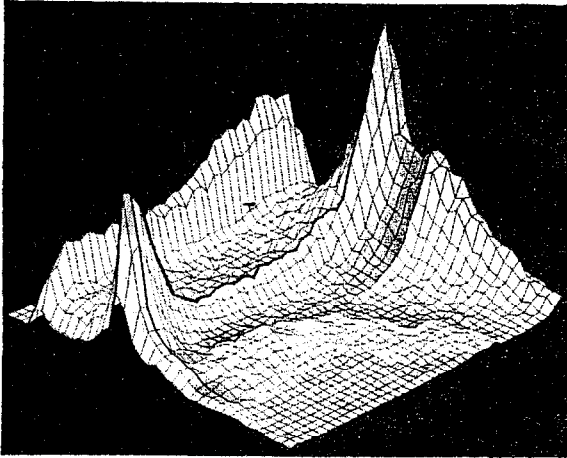


Fig. 7. Apparent 3-d plot of the invariant $K\pi$ mass ($M_{K\pi}$) versus the t-channel decay angle of the K in the $K\pi$ center of mass ($\cos \theta_J$). The axes in the plane are: $.7 < M_{K\pi} < 2.5$ GeV along the lower left-hand side; and $-1.0 < \cos \theta_J < 1.0$ along the lower right-hand side. The number of events, arbitrarily scaled, is plotted above the plane.

variables in the lower plane are $M(K\pi)$ and the cosine of the t-channel kaon decay angle in the $K\pi$ center of mass ($\cos \theta_J$). The height of the surface above the plane is the number of events per bin arbitrarily scaled. The $K^*(890)$ stands out clearly as a ridge at low mass while two dramatic spikes, at both forward and backward $\cos \theta_J$, signal the 2^+ $K^*(1435)$. As we continue to higher $M(K\pi)$, the structure grows more complex. There is a clear bump in forward $\cos \theta_J$ in the region around 1740 MeV on top of a ridge extending to high mass. This ridge becomes

progressively steeper as $M(K\pi)$ increases and is indicative of $K\pi$ diffractive scattering. It falls off as the mass increases due to a fixed angle cut generated by our two prong trigger. At smaller $\cos \theta_J$, there is a complex plateau structure which peaks at a $\cos \theta_J$ of ≈ -0.5 at about 1800 MeV. As $|Y_{30}|^2$ has a peak at this same $\cos \theta_J$, one might wish to interpret this behavior as being due to the $3^- K^*(1780)$.

Continuing to still higher $M(K\pi)$, the structure grows even more complex. At a mass of about 2100 MeV, there are small peaks at $\cos \theta_J \approx 0$ and $\cos \theta_J \approx -1$ which one might speculate as being due to a high even-spin object such as the 4^+ K^* expected in this mass region. In any event, the obvious interference structure observed in this plot is both a promise and a caution.... The promise that there is a great deal of interesting physics in the data coupled with the

caution that a sophisticated analysis is likely to be necessary to understand the obvious inherent complications. In particular, one must be very cautious about the interpretation of bumps in invariant mass distributions. This is particularly obvious in figure 8, which shows one-dimensional $M(K\pi)$ plots cut in ten different slices of $\cos \theta_J$. The change in apparent width and position of the various structures as one changes $\cos \theta_J$ is very dramatic. For example, the apparent structure in the region around 1800 MeV moves substantially in both mass and width as one moves across the $\cos \theta_J$ region. Note too, that the "shift" effect can be substantial even in the region of a large leading state. One can clearly see a shift of the structure around 1400 for example. The forward and backward peaks are centered at ~ 1435 but the structure becomes quite asymmetric and substantially lower in mass for $\cos \theta_J$ near 0. As I will show later, this effect is due to a non-leading 0^+ wave which peaks just below the 2^+ . In any event, a fit to the projected distributions in $M(K\pi)$ will clearly give a mass value for the 2^+ object which is substantially too low. It was this effect as observed through the earlier partial wave

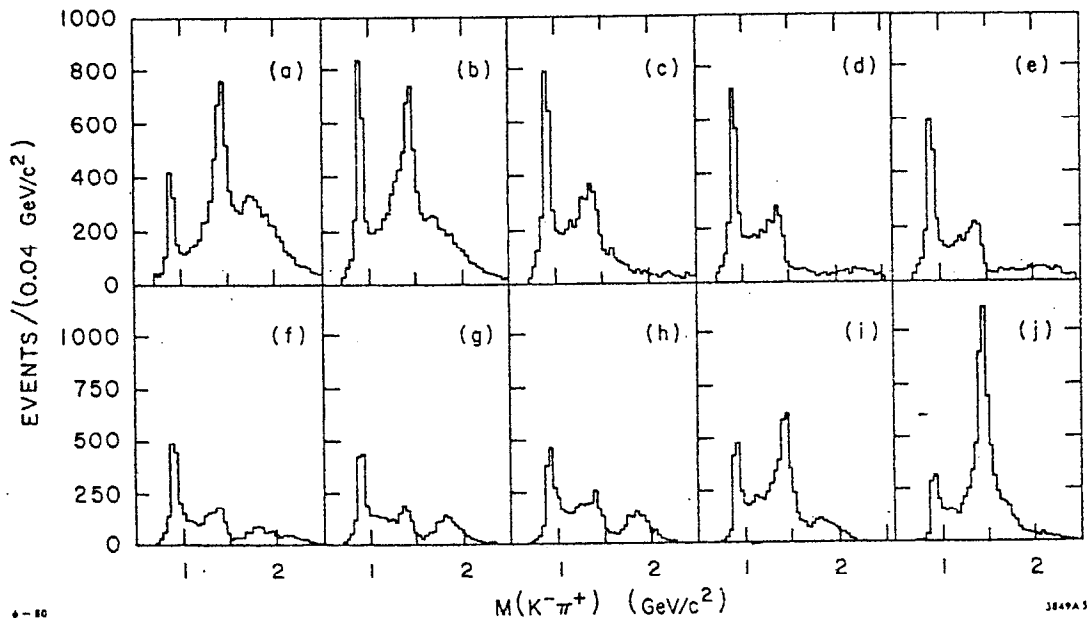


Fig. 8. Invariant $K\pi$ mass spectra cut on 10 different $\cos \theta_J$ slices $|\cdot 2|$ in width. (a) through (j) are ordered from the forward to the backward direction so that, for example, (a) contains the slice $.8 < \cos \theta_J \leq 1.0$ and (j) contains $-1.0 \leq \cos \theta_J \leq -.8$.

analysis of the 13 GeV data,³ and confirmed by the present analysis, which shifted the 2^+ mass from its historical 1420 MeV to the presently accepted value of 1434 MeV.⁹

Having hopefully convinced you that there is a great deal of interesting structure in the $\cos \theta_J$ versus $M(K\pi)$ plot which does not appear clearly as bumps in the invariant mass distribution, let us proceed to look at this structure as observed in the spherical harmonic moments of the decay angular distribution. We select the data for this analysis to emphasize the π exchange contribution by cutting on $|t'| < .2$. We also make tight cuts to remove the small competing background reactions and are left with 51,000 events in the small $|t'|$ region. Figure 9 shows the t-channel $M = 0$ moments for this data. In general, at each mass value they are plotted only up to the smallest value of L_{\max} required to fit the data. The well known $K^*(890)$ and $K^*(1435)$ bumps are apparent, and their spins can be simply confirmed as 1^- and 2^+ respectively from the behavior of the $\langle Y_{20} \rangle$ and $\langle Y_{40} \rangle$ in these mass regions. Note also the interference patterns in the odd L moments as we move through the resonances. As we go to higher mass we see a clear bump in the $\langle Y_{60} \rangle$ at 1780 MeV indicating the $J^P = 3^- K^*(1780)$ state. Continuing still higher in mass, we see a bump structure in the $\langle Y_{60} \rangle$ and $\langle Y_{80} \rangle$ coupled with a classic interference pattern in the $\langle Y_{70} \rangle$. Since higher moments are consistent with zero in this region, we interpret this structure as the next leading $J^P = 4^+ K^*$ required by the quark model.

The probable existence of a large number of underlying states in this region makes a determination of the parameters of this new state rather difficult. At the present time, we have performed a naive fit assuming a relativistic Breit-Wigner in the F and G waves and a simple polynomial background in the D, F, and G waves. After fixing the leading 3^- resonance at values based on our preliminary partial wave analysis results as noted below, we performed a fully correlated fit to the $\langle Y_{60} \rangle$, $\langle Y_{70} \rangle$, and $\langle Y_{80} \rangle$ moments in the region from 1500 to 2300 MeV. We obtain

$$M_F \approx 1790 \text{ (fixed) MeV,}$$

$$\Gamma_F \approx 190 \text{ (fixed) MeV,}$$

$$M_G \approx 2070 \text{ MeV},$$

$$\Gamma_G \approx 220 \text{ MeV},$$

where the errors are dominated by systematics inherent in the assumptions of the model. The significance of the $J^P = 4^+$ state in this model is greater than 4.5σ , and as such, constitutes definitive evidence for a new leading state, the $K^*(2070)$.⁸

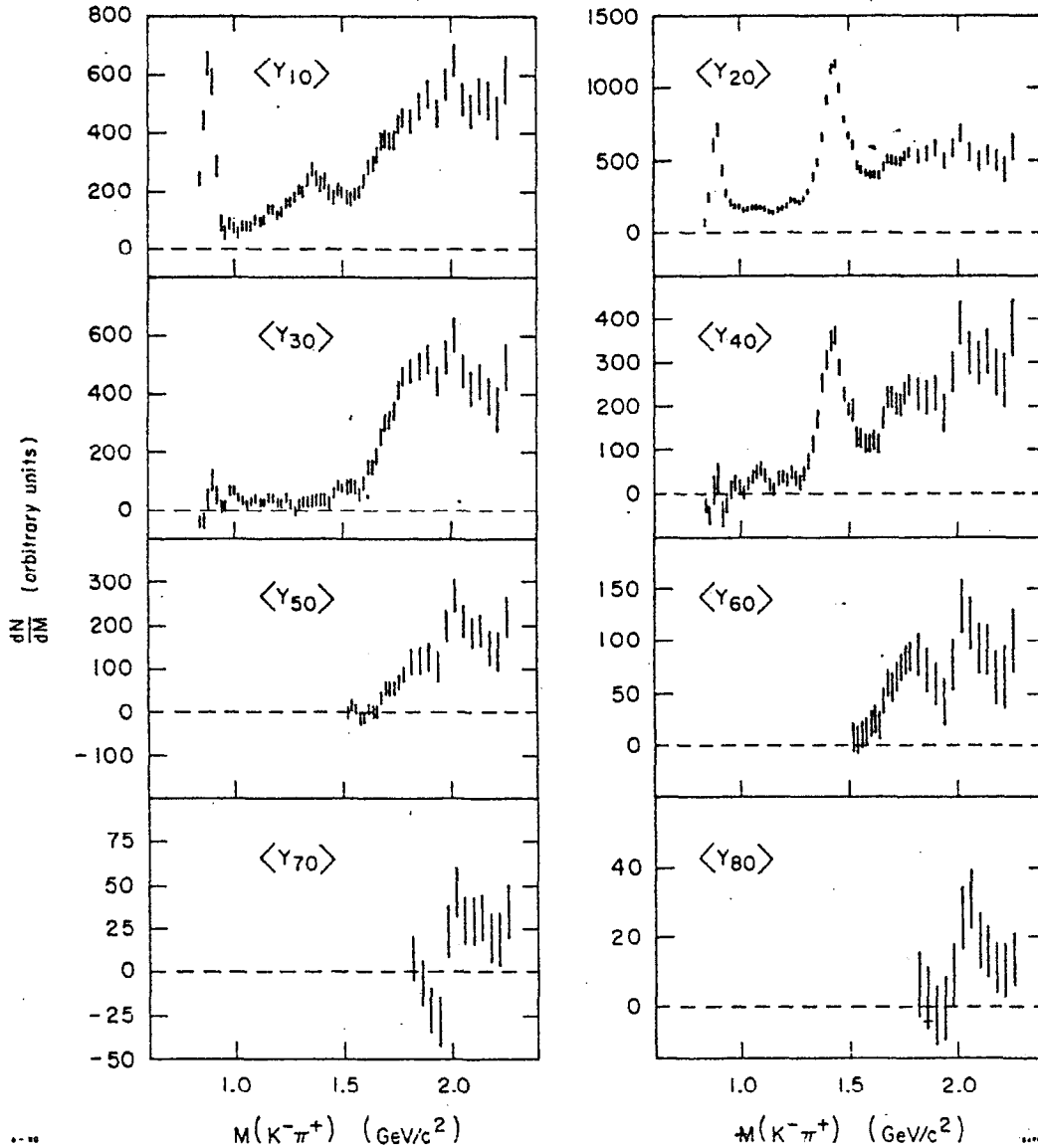


Fig. 9. The unnormalized t -channel moments of the $K^- \pi^+$ angular distribution for $|t'| < .2 \text{ GeV}^2$. The bins are overlapped by a factor of two to guide the eye.

As we have just illustrated, a great deal can be learned about the leading states by studying the mass dependence of the angular moments of the data. In addition, however, the quark model leads us to expect lower lying states in this same region which will be hidden in the interferences seen in the moments. In order to understand these effects, we are in the process of performing an energy independent partial wave analysis. As of today, preliminary results are available to a $K\pi$ mass of 1.84 GeV. This analysis is based on a t -extrapolation to the pion pole of the π -exchange contributions to the t -channel helicity-zero $K\pi$ production amplitudes. It is described in detail in reference 3 so it will not be discussed here. Let me, however, delineate a few of the important assumptions of this analysis: (I) we fit to the smallest number of partial waves required by the data; (II) we constrain the S- and P-waves to be elastic below 1.3 GeV; (III) we assume the $I = 3/2$ wave as given by the 13 GeV SLAC experiment;³ and (IV) we set the overall phase in the inelastic region by assuming the phase of the leading state is given by a relativistic Breit-Wigner.

In general, the results obtained are quite consistent with our earlier 13 GeV analysis. However, the errors are smaller (and the features therefore clearer) in the high mass region due to the substantially better acceptance. As I will show below, one particularly important consequence of this is that there is only a single unambiguous solution below ~ 1700 MeV which, therefore, determines the existence of the observed structures uniquely.

The S- and P-waves for this solution are shown in figure 10. In addition to the leading $1^- K^*(890)$ resonances, there is interesting additional structure indicative of non-leading resonance-like effects. The S-wave exhibits a smooth slow rise in both phase and magnitude until 1.3 GeV. The magnitude then rises rapidly followed by a precipitous drop in the region just above 1.4 GeV. This is coupled with a rapid change in the phase motion indicating resonance behavior. As the mass continues to increase the magnitude becomes very small and the phase becomes indeterminate. Both the magnitude and phase then begin to move again but, unfortunately, right at the end point of the

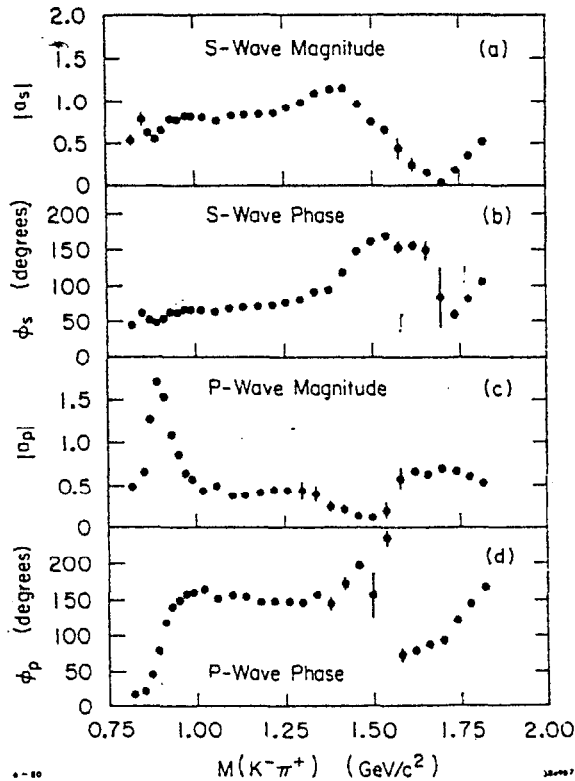


Fig. 10. The S- and P-wave $K\pi$ scattering amplitudes from the reaction $K^-p \rightarrow K^-\pi^+n$. See text for a full explanation.

with the non-leading S- and P-wave features described above. In particular, the S-wave wanders up slowly from low mass, passing through 90° at about 1300 MeV, but with very little evidence of resonance behavior there. However, at about 1450 MeV, we see an essentially elastic S-wave loop which is relatively narrow (perhaps 250 MeV) looking very much like a resonance. The P-wave amplitude traces out the elastic $K^*(890)$ resonance and then curls around relatively quickly in the region around 1650, again indicating resonance-like behavior.

One of the most exciting features of the present analysis is the indication that it is unambiguous below ~ 1700 MeV. The ambiguities are most readily apparent as an indeterminacy in the signs of the imaginary parts of the complex zeros of the scattering amplitudes which were emphasized by Barrelet.¹⁰ Since elastic unitarity allows

present analysis. In the P-wave we see the expected elastic $K^*(890)$ resonance, with little happening above that until about 1500 MeV. The magnitude is very small here, but rises to a broad peak centered around 1.7 GeV. This rise is accompanied by a fairly rapid phase variation again indicative of resonance-like behavior.

The $K\pi$ partial waves as shown in figure 10 are perhaps easier to interpret when plotted as Argand diagrams. Figure 11 shows the clear circular motion expected for the leading 1^- , 2^+ , and 3^- waves. We can also see motion associated

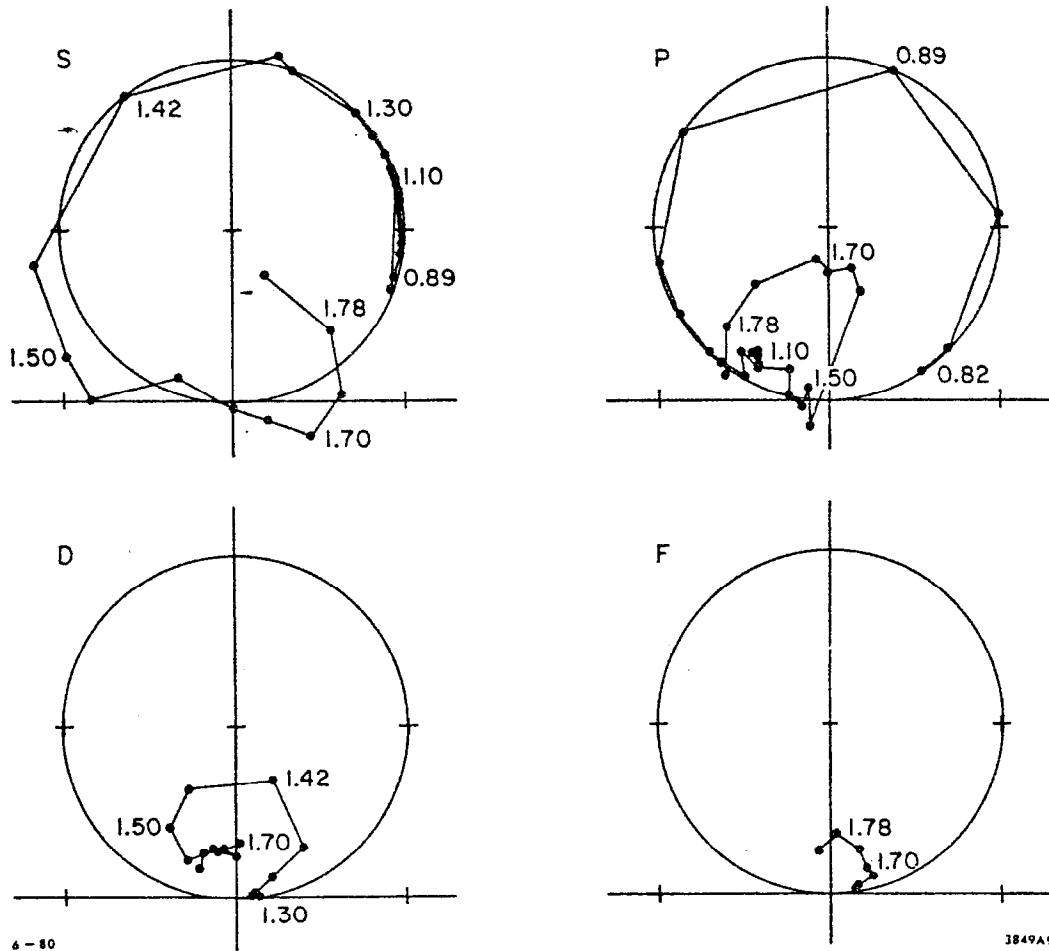


Fig. 11. Argand plots for the $I = 1/2$ $K\pi$ partial waves. The $I = 1/2$ S-wave was obtained by subtracting the $I = 3/2$ S-wave amplitude determined in the 13 GeV K^\pm experiment from the full S-wave amplitude. The $I = 3/2$ components of the other waves are neglected. See text for a full explanation.

only one solution below 1 GeV, no ambiguities arise until one of the zeros becomes small. Figure 12 shows the real and imaginary parts of the three zeros plotted with error estimates. None of the imaginary parts of the zeros appear close enough to the axis to change signs in the region below 1700 MeV. Hence, we conclude that there is a unique solution in this preliminary analysis.

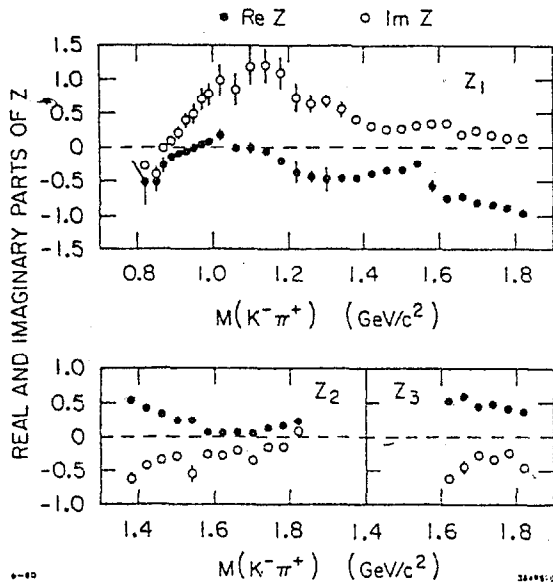


Fig. 12. The real and imaginary parts of the complex zeros of the $K\pi$ scattering amplitudes. Note that the error bars lie within the point diameters unless shown.

V. CONCLUSION

The $K\pi$ moments clearly show the "old" leading K^* resonances; the 890 (1^-), 1435 (2^+), and 1780 (3^-). In addition, a new 4^+ resonance is observed at about 2070 MeV, which is naturally interpreted as a SU(3) partner of the h meson. Preliminary results from a $K\pi$ partial wave analysis in the mass region below 1840 MeV clearly confirm the 1^- , 2^+ , and 3^- resonances. The most interesting new result is that this analysis has no ambiguities below 1700 MeV so that the evidence for resonance behavior of the nonleading 0^+ wave at about 1450 MeV and the 1^- wave at about 1650 is also unambiguous.

These results and those reviewed earlier today⁷ demonstrate the usefulness of having very high statistics data in different channels. We have a great many final states in this experiment most of which are just beginning to be analyzed. We will be extending the data sample by about a factor of seven during the next year, and are looking forward to a productive investigation of the properties of states containing the strange quark during the next few years.

ACKNOWLEDGMENTS

I would like to thank my fellow collaborators and the technical staffs of SLAC Group B, Carleton University, and the LASS Operations group on whose efforts this talk is based. Special thanks are due David Aston, Stan Durkin, Alan Honma, William Johnson, David Leith, and Robert Richter for invaluable help in preparing the specific material of this talk.

REFERENCES

1. See, for example, G. W. Brandenburg, R. K. Carnegie, R. J. Cashmore, M. Davier, T. A. Lasinski, D.W.G.S. Leith, J.A.J. Matthews, P. Walden, and S. H. Williams, Nuclear Physics B104: 413, 1976.
2. G. W. Brandenburg, R. K. Carnegie, R. J. Cashmore, M. Davier, W. M. Dunwoodie, T. A. Lasinski, D.W.G.S. Leith, J.A.J. Matthews, P. Walden, S. H. Williams, F. C. Winkelmann, Physical Review Letters 36:703, 1976.
3. P. Estabrooks, R. K. Carnegie, A. D. Martin, W. M. Dunwoodie, T. A. Lasinski, and D.W.G.S. Leith, Nuclear Physics B133:490, 1978.
4. D. Aston, W. Dunwoodie, S. Durkin, A. Honma, W. B. Johnson, P. Kunz, D.W.G.S. Leith, L. Levinson, B. N. Ratcliff, R. Richter, S. Shapiro, R. Stroynowski, S. Suzuki, G. Tarnopolsky, S. Williams, N. Horikawa, S. Iwata, R. Kajikawa, T. Matsui, A. Miyamoto, T. Nakanishi, Y. Ohashi, C. O. Pak, T. Tauchi, T. Shimomura, K. Ukai, and S. Sugimoto, SLAC-Proposal-E/135, October 1979.
5. D. Aston, W. Dunwoodie, S. Durkin, T. Fieguth, A. Honma, D. Hutchinson, W. B. Johnson, P. Kunz, T. Lasinski, D.W.G.S. Leith, L. Levinson, W. T. Meyer, B. N. Ratcliff, R. Richter, S. Shapiro, R. Stroynowski, S. Suzuki, S. Williams (SLAC), R. Carnegie, P. Estabrooks, R. Hemingway, R. McKee, A. McPherson, G. Oakham, J. Va'Vra (Carleton University and National Research Council, Ottawa).

6. P. F. Kunz, R. H. Fall, M. F. Gravina, J. H. Halperin, L. J. Levinson, G. J. Oxoby, Q. H. Trang, SLAC-PUB-2418, October 1979.
7. R. Cashmore, invited talk at this conference; The VI International Conference on Experimental Meson Spectroscopy, Brookhaven, April 1980.
8. Evidence for a charged spin-four K^* state at 2060 MeV has been presented by C. Nef, this conference; The VI International Conference on Experimental Meson Spectroscopy, Brookhaven, April 1980.
9. Particle Data Group, LBL-100, April 1978.
10. E. Barrelet, Nuovo Cimento 8A:331, 1972.